

PRACTICAL INFLUENCES OF GEOMETRIC AND RADIOMETRIC IMAGE QUALITY PROVIDED BY DIFFERENT DIGITAL CAMERA SYSTEMS

By S. ROBSON*

University College London

and M. R. SHORTIS

University of Melbourne

(Paper read at the one-day symposium of the Photogrammetric Society, entitled *The Development and Application of Industrial Photogrammetry*, on 25th November, 1997)

Abstract

Imaging systems founded on current digital camera technology are finding widespread use in high precision measurement applications. A single digital CCD camera, or an array of such cameras, equipped with ring lighting equipment is commonly used to acquire imagery of high contrast retroreflective targets placed on the object at discrete locations to signalize points of interest. The precise and accurate measurement of each imaged target location is a fundamental requirement if suitable measurement tolerances are to be obtained. Whilst such systems are undoubtedly capable of producing excellent results, the practical effects of target image quality on the photogrammetric measurement process is in need of careful consideration. This paper revisits some fundamentals of the optical imaging of retrotargets and investigates some abilities of a range of digital camera systems to provide images of retrotargets that are appropriate to the measurement process. Some experimental results are presented including the imaging of planar arrays of differing sized retrotargets at differing angles and exposures and a series of network analyses in which the level of target image intensity has been varied systematically.

KEY WORDS: digital camera, image quality, retroreflective targets

INTRODUCTION

RECENT ADVANCES in digital imaging technology coupled with automation in data processing have, as a response to market forces, brought digital photogrammetry into

*Formerly at City University, London.

routine non-expert use for high precision engineering measurement (Brown and Dold, 1995; Beyer, 1995; Bösemann and Sinnreich, 1994). End user expectations not only include rapid measurement and ease of system use, but also routine achievement of given measurement specifications. To achieve this latter aim, co-ordinate measurement data must be assessed according to their accuracy, precision and reliability. Precision (random error) and reliability (susceptibility to gross error) are routinely assessed within the almost universally accepted bundle adjustment process (Granshaw, 1980). Assessment of accuracy is however more difficult since it is concerned with systematic error within the measurement volume and requires independent spatial information of appropriate and verifiable quality. The results of work to evaluate photogrammetric procedures in association with established metrological procedures have demonstrated significant variations between achieved accuracy and estimated precision (Shortis, Snow, and Goad, 1995; Fraser and Shortis, 1995). It is evident that conformance to standards requires an international research effort if a specification and the methodology necessary to verify accuracy under practical conditions are to be achieved.

The increasing importance of data quality verification has been brought about by the ability of digital camera systems and retrotargeting methods to produce high quality spatial data in a user friendly manner under a wide variety of industrial and engineering applications. As it becomes increasingly accepted that the technology is mature, it is necessary to ensure that the processes of imaging retrotargets onto CCD arrays, target image measurement and the photogrammetric mathematical model used are sufficiently understood and appropriately implemented. Whilst much work has been carried out in this area, the content of this paper is directed towards evaluating some radiometric and geometric image quality issues that are less frequently reported and have a direct and significant bearing on the retrotarget measurement process. In particular, the paper aims to highlight some practical imaging performance issues within the photogrammetric process which are not yet adequately understood or mathematically modelled. Some effects of these largely systematic processes are described with reference to tests conducted using several different digital camera systems that are representative of current technology.

SOME FUNDAMENTALS OF RETROTARGET IMAGING

It is not reasonable in a single paper to discuss and evaluate all aspects of retrotarget imaging and target image measurement. The discussion in this paper is limited to several discrete key areas that are considered important to the geometry and radiometry of retrotarget imaging and worthy of a more complete understanding. These include a questioning of the application of some basic geometric assumptions and a brief consideration of lens aberrations and lens design, and their effect on the imaged shape of retrotargets at the centre and edges of the field of view.

Reported Retrotargeting System Performance

The key to retrotarget image measurement is the ability to estimate the centre, according to the geometrical model of point to point projection, of each imaged target to subpixel accuracy. There are two tasks to be performed in this process: recognition and location. Recognition of the target images is required to unambiguously identify targets within a scene and provide a coarse location for a local window or boundary. The precise location of the target image is generally a second process that determines the target image position within that local window or boundary.

Coarse locations can be determined using prior geometric knowledge of exposure station and target positions (Haggrén and Haajanen, 1990), scanning the

entire image based on a global threshold (Shortis *et al.*, 1994) or searching for coded targets (van den Heuvel *et al.*, 1992). Once located, target image centres can be computed using intensity weighted centroids (Trinder, 1989), edge detection and ellipse fitting (Zhou, 1986), or least squares template matching (Baltasvias, 1991). Centroids and ellipse fitting require the elimination of background or noise by the definition of a local threshold. Whilst template matching may be independent of high contrast targets, the technique requires an initial template to be defined and can become computationally inefficient unless there are sufficient algorithmic constraints (Gruen and Baltasvias, 1988).

Analysis by simulation can predict the expected image space precision of target centring algorithms. Most studies are based on assumptions of grey scale imagery, random noise and minimum target spans of a few pixels. The consensus is that centroid type algorithms can at best realize image space precisions of ± 0.01 pixels (Stanton *et al.*, 1987). There have been many tests of image space precision of target centring algorithms. Chosen test methods vary from single target monitoring (Robson *et al.*, 1993) to multistation convergent networks comprising many targets (Shortis, Clarke and Robson, 1995). The consensus is that centroid type algorithms can realize object space precisions equivalent to ± 0.02 to 0.03 pixels. Few tests have included verification in the object space. Of those reported, object space results have generally been less favourable, indicating imaging accuracies of ± 0.02 to 0.07 pixels (Fraser and Shortis, 1995). Whilst subpixel measurement techniques undoubtedly produce good results, it is prudent to consider what factors affect the geometry and radiometry of the digital image intensity distribution that is being measured.

Potential of Optical Distortions for Retrotarget Measurement Error

In order to form a retrotarget image at the CCD sensor, light must travel from a suitable illumination source, be efficiently returned by the target material and be collected and focused by the lens system onto the CCD array. The optical path may include additional glassware such as a CCD cover glass or condenser optics. In as much as the illumination of retrotargets (Brown, 1984) and the response qualities of CCD arrays are well reported (Shortis and Beyer, 1997), the influences of the optical image formation processes are less well published in photogrammetric literature. Further, as differences between accuracy and precision estimates demonstrate, whilst established photogrammetric procedures are sufficient for most work, the continual improvement of CCD sensor systems and the automation of data capture are exposing some shortcomings.

(i) *Some geometric considerations.* Photogrammetrists have traditionally represented the imaging process by means of collinearity and a parametric model to represent the geometry of the camera. In accordance with this tradition, it has been convenient, and with qualified success, to consider retrotargets as a point source. This consideration is generally taken to be a good approximation for targets that produce images of the order of 3 pixels to 5 pixels in diameter. Such a target image diameter allows optimum subpixel measurement accuracy. Larger target images require that the significance of perspective projection be considered (Dold, 1996). According to central perspective projection, a circular target of diameter D aligned parallel to the image plane will be imaged as a circle of diameter d (Fig. 1). If, however, that target is aligned orthogonally to its image ray, then its imaged diameter will be a function of the angle θ subtended to the optical axis. Furthermore, its true centre will not coincide with its imaged centre as determined by a centroiding procedure but will have some radial offset, the size of which will depend upon the target diameter,

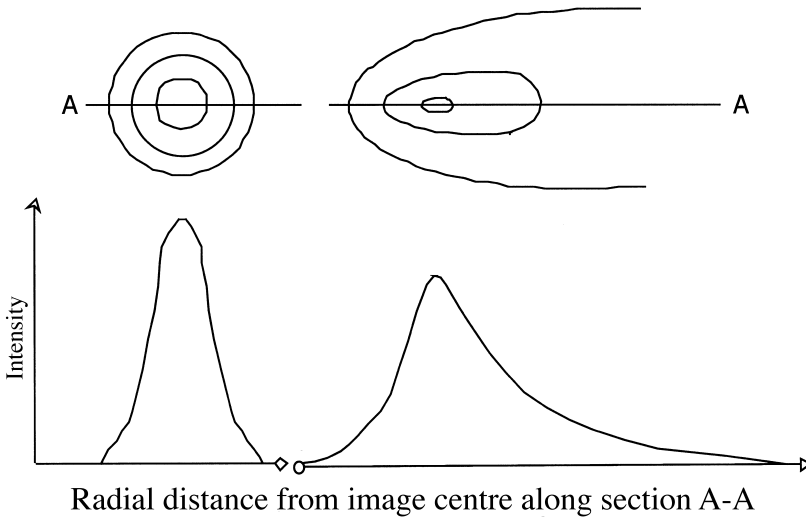


FIG. 2. Lens point spread function at the format centre and its change in shape with radial distance to the edge of the field of view.

Photogrammetrists have generally made use of rectilinear lenses that are designed to reproduce straight lines in the object space as straight lines in the image space according to the function: radial distance, $r = f \tan \theta$ (Fig. 3). Necessitated by available digital camera designs and the relatively small image format size of CCD arrays, it is common to use lenses of short focal length for digital photogrammetric work. However, short focus lens designs can only provide a small clearance between the vertex of the rear element and the focal plane. This limitation can present particular problems with cameras based upon 35 mm SLR style bayonet mounts where lens design is influenced by the necessity to allow for a mirror viewing system between the rear elements of the lens and the image plane. In such cases, lenses of retrofocus design are employed. This type of design shifts the front and rear nodal planes backwards to allow a larger physical separation between the lens rear element and the image plane, thereby providing sufficient back focal distance for mirror clearance. Unfortunately, retrofocus lens designs typically have larger geometric distortions than their more symmetrical short focus counterparts and may contain very steeply curved elements and high refractive index glass. This combination of design criteria can also make such constructions prone to flare. Additionally, uniform lens performance in the corners of the format is difficult to achieve in practice due to difficulties of centring the elements in assembly (Ray, 1994).

One possible alternative is to consider the use of so called fisheye and quasi-fisheye lenses (Welford, 1974). In such designs, the ability to record straight lines in the image space is sacrificed for improved image illumination. Whilst several methods of projection are possible, that most commonly found is based upon radial distance, $r = f \theta$ (Fig. 3). Since the designed change in imaging geometry is a function of image radius, it is possible to mathematically model the imaging geometry of the fisheye projection with established radial lens calibration parameters. As a point of interest, the term fisheye is used where the image circle is wholly within the image format (a) whilst quasi-fisheye lenses generally achieve a 180° field of view across their designed image format diagonal (b).

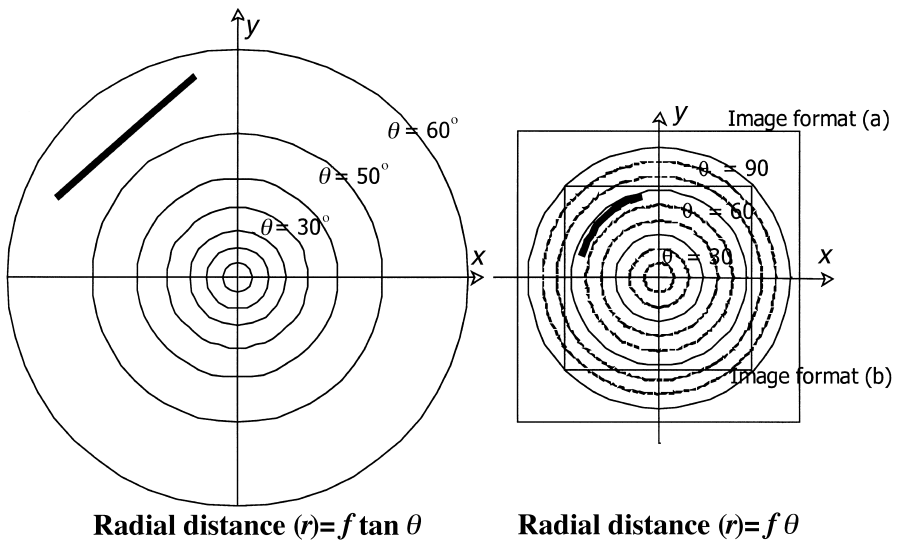


FIG. 3. Conventional rectilinear projection and a fisheye lens projection.

One final optical consideration is the effect of additional glass, such as CCD cover glasses. These may be unflat, non-orthogonal to the optical axis or both. The inclusion of such additional elements in the optical system is likely to result in image shifts and an increase in aberration, particularly coma.

CCD ARRAYS AND DIGITAL CAMERA SYSTEMS

Digital camera systems in common use for photogrammetric measurement purposes include those from more broad based manufacturers such as Kodak, Pulnix, Sony and Hitachi. Such cameras are intended for the general market, photojournalism and, to a lesser extent, scientific applications such as medicine and machine vision. Also available are purpose built photogrammetric cameras from, for example, Leica/GSI, Aicon, Rollei and Zeiss. Primary imaging features connected with selecting a digital camera appropriate to retarget image acquisition are: CCD characteristics, lens mount, mechanical stability, method of data transfer, the ability to synchronize to an external electronic flash and, depending on application, the ability to synchronize image capture between multiple cameras.

CCD Arrays and Digital Data Transfer

The fundamental function of any solid state sensor is the absorption of light photons by the sensor material and subsequent conversion into an electric signal in the form of charge. Charge transfer and read out are implemented in the form of the charge coupled device or CCD. Current imaging technologies for mainstream uses are centred around interline and frame transfer CCD arrays and the increasingly more common progressive scan technology. Specialist cameras can also utilize micro-scanning and/or macro-scanning where the light sensitive array is incrementally moved to effectively increase resolution or image format size. This paper is limited to a discussion of frame transfer and progressive scan models utilizing digital output.

(i) *Types of CCD sensor.* CCD sensors have different types of logical organization for imaging and read out. Frame transfer CCD sensors have imaging areas that are composed only of sensor elements. In contrast to an interline sensor, the same sensor elements are used for charge accumulation and for charge transportation. The light sensitive portion of the array must therefore be masked either mechanically or electronically during the columnwise charge transfer process. Frame transfer sensors are common for high resolution and so called scientific cameras, whilst standard closed circuit television and video cameras are dominated by interline transfer sensors which are more compatible with video recording systems.

Traditional CCD cameras are only capable of capturing one field, or half the vertical information, per shutter event because the scan function breaks the integration period into two sequential field scans. In dynamic image capture, by the time the second field of information is stored and scanned, the subject may have moved. The result is a ghosting or blurring effect once the two scan periods are combined to create the whole, interlaced picture. This is successfully eliminated with progressive scanning where the image information is accumulated simultaneously and then output either line by line or sequentially. The result is a non-interlaced image with full vertical and horizontal resolution captured in a single rapid shutter event (Hori, 1995). The disadvantage of this type of camera is that image acquisition at field rate is not possible, but this is balanced against the clear advantage of frame rate images which are free of motion blur. Both the Kodak ES1.0 and Pulnix TM9701 cameras, evaluated later in this paper, utilize progressive scan technology.

Consistent and regular image geometry is a prerequisite requirement for accurate image measurement. Commonly, transfer from the CCD array to a frame grabber requires an analogue to digital (A/D) converter. In such cases, timing errors between CCD array and A/D converter can give rise to synchronization error or line jitter (Raynor and Seitz, 1990). Such problems are eliminated in digital cameras where the A/D converter is matched to the CCD array and driven by the same timing generator. In a digital camera, output to the user is typically provided via a digital interface. One such example is the RS422 high speed parallel interface which requires a compatible interface board in the host computer. Digital transmission errors will result in an obvious missing frame, or an offset frame being loaded into the image memory, rather than more subtle geometric errors.

(ii) *Some opto-electronic considerations.* The mechanical and electronic characteristics of the CCD sensor and its associated electronics determine the fidelity with which the image formed by the optical system is converted into a computer readable format. Many of the issues connected with CCDs and the electronics used in digital cameras are beyond the scope of this paper, which is limited to a brief consideration of the effect of pixel geometry, read out noise and blooming which are particularly apparent in some of the camera systems tested. The reader seeking more general detail is referred towards Shortis and Beyer (1996).

CCD sensors are fabricated by deposition of a series of layers on the silicon substrate. The geometry of the deposited layers is controlled by photolithography, which uses masks prepared at a much larger size than the finished product and applied using optical or photographic reduction techniques. The limit of geometric accuracy and precision of CCD sensors can be deduced from the accuracy and precision of the lithographic process. The current generation of microprocessors is fabricated to 0.3 μm to 0.5 μm design rules, which require alignment accuracies of better than 0.1 μm . This alignment accuracy is supported by Pol *et al.* (1987) who suggest the possibility of local systematic effects of 1/60th and an r.m.s. error of 1/100th of the sensor element spacing on an 8 mm square format. It could be expected that these

1/60th to 1/100th levels of fabrication error would also hold for larger format sensors due to the nature of the lithography process.

A further criterion is that of a match between the resolving power of the optical system and that of the CCD array. Any mismatch will give rise either to aliasing if the array has greater resolution than the lens or, in the converse case, a general loss of resolution will result (Lenz and Fritsch, 1988). It is important to note that, due to varying CCD construction, resulting in differences in pixel pitch and the percentage light sensitive area or fill factor of each pixel, sensor resolving power may not be homogeneous in the x and y directions. Such variations can be expected to have an influence on the geometric shape and intensity profile of retrotarget images.

Following practical experience, the predominant concerns in this paper are readout effects and blooming. These effects are apparent when too much light falls onto a sensor element or group of sensor elements and the finite charge capacity of the photosensitive sites is approached or exceeded. The excess charge then spreads into neighbouring elements, falsely increasing the apparent image intensity. The effect is known as blooming and is most commonly associated with intense light sources, such as the response of retroreflective targets to an electronic flash. Blooming can be readily detected by the excess spread of such light sources in the image, or image trails left by excess charge during read out.

Although blooming cannot be totally eliminated from CCD sensors, the inclusion of so called antiblooming drains has dramatically reduced the problem. Antiblooming structures typically use additional electrodes and channel stops between the photosensitive sites on the array to drain off excess charge (above a set threshold potential) into the base substrate material of the CCD. The additional circuitry reduces the light sensitive area of each pixel, typically from 100 per cent with no antiblooming to approximately 70 per cent with antiblooming for a frame transfer sensor. As it is easier to prevent blooming across columns with the drain structures, blooming usually occurs within columns first.

Blooming has an interim stage characterized by retrotarget images exhibiting small "tails" aligned in the read out direction within columns. The tails may be in the vertical or horizontal direction in the image, depending on the column direction of the CCD array. This read out effect is caused by the centre of the retrotarget, the most intense part of the image, blooming and the excess charge spilling over into neighbouring sensor elements, initially in the column direction. At higher illuminations, the more general case of blooming ensues, in which the excess charge is so great as to affect surrounding sensor elements in all directions. However, as is shown in Fig. 6, even in cases of dramatic blooming the principal effect remains in the read out direction, corresponding to columns in the CCD architecture.

Whereas initial attempts at antiblooming could control illumination levels only up to 100 times the saturation exposure, the limit has risen steadily to attain levels of over 10 000 times the saturation level of the sensor in current consumer products (Kodak, 1995). Unfortunately, antiblooming structures occupy areas on the CCD surface which would otherwise be light sensitive, hence reducing fill factor and compromising sensor resolution. Such problems can be addressed by the use of microlens arrays. These arrays are designed to collect the majority of the light falling on the sensor and focusing it onto the light sensitive areas of the pixels.

Available Digital Camera Systems

Camera systems investigated for this paper were selected according to availability and include a monochrome Kodak DCS420, MegaPlus 1.6IAB, MegaPlus ES1.0, Pulnix TM9701 and a GSI INCA camera which is based on the Kodak MegaPlus 4.2I camera body. The cameras are drawn from the three principal

TABLE I. Manufacturers' figures, where available, for the cameras tested.

Camera	Image size		Pixel size (μm) (Pixel fill %)		Active image dimensions (mm)		Signal/ noise (dB)	Equiv. ISO	Max. frame rate (fps)	Min. exposure (s)
	Rows	Cols.	Width	Height	Width	Height				
Pulnix TM9701	768	484	11.6	13.6	8.91	6.58	50	—	30	1/16 000
MegaPlus ES1.0	1008	1018	9 (60)	9 (60)	9.07	9.16	56	400–1500	30 (T) 15 (S)	1/8 000 (1/16 000)
MegaPlus 1.6I	1536	1024	9 (100)	9 (100)	13.8	9.2	65	100–1500	5.46	1/1 000
MegaPlus 1.6LAB			9 (70)	9 (100)						
DCS420			9	9	13.8	9.2	—	100–800	—	1/8 000
MegaPlus 4.2I	2029	2044	9 (100)	9 (100)	18.5	18.5	65	100–1500	2.1	1/1 000

categories of domestic/photojournalism, scientific/tethered cameras and purpose built photogrammetric cameras. Some pertinent details from their published specifications are given in Table I.

The Kodak DCS420 is a self-contained camera intended for photojournalism and non-specialist photography utilizing storage based on flash memory cards or PCMCIA hard disk drives and an integral power supply. The camera allows a predefined number of images to be stored per card which can then be downloaded onto a host computer when convenient.

The Kodak MegaPlus 1.6I, MegaPlus ES1.0, and Pulnix TM9701 belong to the scientific category. The Kodak MegaPlus 1.6I employs a frame transfer CCD array, whilst the others utilize progressive scan architecture. All of these cameras must be directly linked to a computer system that, if by wire, must be within a radius of no more than approximately 10 m. The Kodak ES1.0 employs a twin tap CCD array to facilitate rapid image to host transfers of up to 30 frames per second.

The most recent advance in photogrammetric camera design is the introduction of “intelligent” cameras (Dold, 1998). The GSI INCA series, as used in the V-STARS industrial metrology systems, includes an onboard processor which searches each image as it is captured. Using a LAN interface, the local processor can communicate the status of an image to the host computer immediately, identifying for example electronic flash failures, lack of coded targets, or lack of an orientation device. Rather than always transmitting the full image, the camera can send a status message, the location of a hand held probe or the entire image. Whilst such systems offer significant benefits, particularly towards automation, the primary consideration with such a camera must still be its imaging performance.

Available Lens Systems

As already noted, the choice of an “off the shelf” digital camera system can place restrictions on the availability of suitable optics. In particular, the small image format of affordable CCD arrays require lenses of short focal length to achieve the wide angles of view common in efficient photogrammetric network designs. The cameras available for the tests carried out in this paper use either “C” mount or conventional 35 mm SLR camera bayonet lens mounts. “C” mount lenses tend to be purpose made for the burgeoning CCD surveillance camera systems market. As a consequence, appropriate well constructed manual fixed focus lenses tend to be in the

TABLE II. Some characteristics of the camera and lens combinations used.

Camera	Lens	Field of view (degrees)			Equiv. 35 mm focal length	Lens construction	Lens mount
		Horizontal	Vertical	Diagonal			
TM9701	9 mm f/1.4 Fujinon	52.3	40.2	63.6	34	Retrofocus	C
ES1.0	10mm f/1.6 Kern-Paillard	48.8	49.2	65.6	33	Quasi-symmetrical	C
ES1.0	12.5 mm f/1.8 Fujinon	41.8	40.2	54.5	41	Retrofocus	C
1.6I AB	15mm f/3.5 Nikkor	49.4	34.1	57.8	38	Retrofocus	Nikon F
1.6I AB	16 mm f/2.8 Nikkor	46.6	32.0	54.8	41	Fisheye	Nikon F
1.6I AB	20 mm f/2.8 Nikkor	38.0	25.8	45.0	51	Retrofocus	Nikon F
DCS420	20 mm f/2.8 Nikkor						
INCA	17 mm f/3.5	56.6	56.8	74.7	28	Not confirmed	Custom

minority. Available 35 mm bayonet mount lenses of short enough focal length to obtain sufficient object coverage with CCD image formats are of retrofocus wide and super-wide angle construction in order to allow for the mirror box viewing assembly incorporated within 35 mm SLR cameras. Additional but more unusual possibilities are offered by fisheye and quasi-fisheye lenses. Some pertinent details concerning the lenses available to the authors are given in Table II.

EXPERIMENTAL WORK

For convenience, practical tests have been divided according to those restricted to two dimensional (2D) measurement of carefully aligned single images and those making use of image networks of three dimensional (3D) target arrays. Single image experiments include an evaluation of target image response and geometric uniformity with reference to a planar array of differing sized retrotargets under a variety of illumination conditions. Work in object space was confined to looking at the effect of variation in target image quality on geometric performance with respect to a 3D target array imaged under a variety of exposure conditions. In the specific case of the Kodak MegaPlus 1.6I camera, the performance of a conventional rectilinear lens has been compared with that of a quasi-fisheye lens of similar focal length.

Image Space Quality Tests

All image space quality tests consisted of imaging a planar array of differing sized retrotargets. The use of such an array allowed the testing of both target shape and exposure uniformity over a range of lens apertures, exposure times and illumination types. The test array at City University was located on a blackened wall and comprised 12 columns of four different sized targets 2.3 mm, 3.2 mm, 5.3 mm and 8.8 mm in diameter. Given appropriate camera alignment and rotations, the array of targets could be arranged to provide images across the format diagonal of each lens and sensor combination. Cameras tested using this array included the MegaPlus 1.6IAB, MegaPlus ES1.0 and a Nikon FE 35 mm SLR film camera. The target configuration used at the University of Melbourne was imaged with the Pulnix

TM9701, Kodak DCS420 and GSI INCA cameras. It included an array of 6.4 mm and 9.5 mm diameter targets arranged on a baseboard as well as other discrete targets located on a laboratory wall.

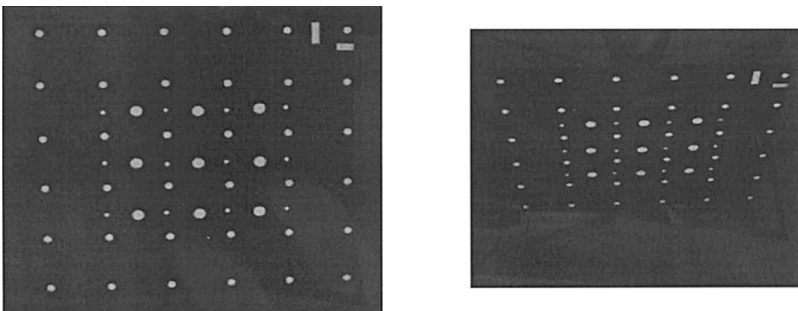
During all tests it was paramount that each lens was correctly focused. This was achieved by opening up the lens aperture to provide an overexposed image in which retrotargets appeared as grossly enlarged discs. The lens was then focused to minimize the size of these target images.

Illumination for each test was provided by a single SunPack DX12R electronic ring flash. When equipped with an external power pack, this unit is able to recycle on low power at better than one flash per second, reducing to a 3 s interval between flashes at full power. Stocker and Yale high frequency fluorescent ring lights were used with the Pulnix TM9701 and Kodak ES1.0 progressive scan cameras. These units are able to provide a continuous and variable ring illumination suitable for retrotarget use at close range when it is necessary to capture images at frame rates greater than those attainable by low cost electronic flash units.

In order to enable a better appreciation of the distinction between CCD effects and those of the differing lenses tested, a comparison using photographic film was also conducted. This test was provided by imaging the target array with a 35 mm Nikon FE camera loaded with Kodak TMAX 100 film and fitted with the same lenses as those used with the "F" mount Kodak MegaPlus camera. Convenient comparisons could then be made by scanning the 35 mm film in a Leica DSW100 scanner. A pixel spacing of 15.0 μm was used for all image scanning.

(i) *Target image shape tests.* This first series of tests was conducted to ascertain the performance of the various systems in imaging retrotargets of various sizes and at differing angles. Having determined a correct exposure level, variations in illumination intensity, lens aperture and exposure time were made in an attempt to introduce readout and blooming in each system. Whilst many megabytes of image data were captured, results can be summarized with reference to a few specific cases.

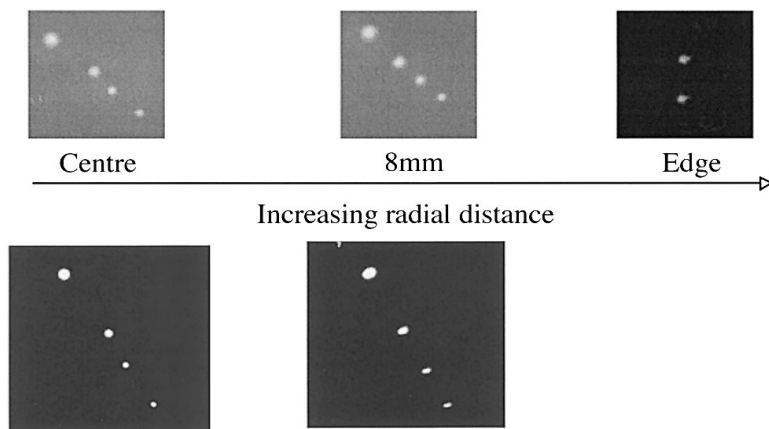
A qualitative example of some of the variations in target shape and size predicted by perspective projection are given in Fig. 4. Both images were taken at the University of Melbourne with a Pulnix TM9701 camera equipped with a Stocker and Yale ring light. For the first image in this figure, the camera was positioned so that its image plane was approximately parallel to the target array, whilst for the second the array was rotated to provide an angle of 50°. The ellipsoidal shape of the oversized targets in the second tilted image is readily apparent.



Images taken from the centre of the format of a Pulnix TM9701 fitted with a 9 mm f/1.4 Fujinon lens.

FIG. 4. Demonstration of change in target shape and size with differing angle.

Target images taken with a 15mm Nikkor lens onto TMAX 100 35mm film



Target images taken with a 15mm Nikkor lens onto a 1.6I AB sensor

FIG. 5. Images of an array of retrotargets of differing size made onto photographic film and a CCD array with the same 15 mm Nikkor lens.

Fig. 5 shows small portions extracted from images of an array of retrotargets of differing size made onto Kodak TMAX 100 film and a Kodak MegaPlus 1.6IAB sensor with the same 15 mm rectilinear Nikkor lens. The differences in scale are due to the scanner's $15.0\ \mu\text{m}$ pixel size as opposed to the $9.0\ \mu\text{m}$ of the CCD array. Differences in tonality are attributable to the different image formation processes. What are apparent, especially for small targets, are the systematic differences in target image shape with increasing radial distance. Given that the image plane was approximately aligned to the target array in each case, such variations cannot be due to perspective geometry considerations but appear characteristic of lens aberration. A similar analysis with a 20 mm Nikkor lens yielded similar but less exaggerated results consistent with the expectation from a lens with a less extreme retrofocus design.

Blooming and readout can present a serious source of error if not carefully controlled. Fig. 6 demonstrates a severe case of blooming from a CCD array with near 100 per cent pixel fill factor. Such a severe result was achieved by opening the lens aperture by about four stops above that required to achieve optimum retrotarget images. Significantly, blooming was still readily apparent at only two stops above optimum exposure. The image in Fig. 7 was taken with a MegaPlus 1.6IAB camera. This camera is specified with an antiblooming CCD array which, at the expense of a 60 per cent pixel fill factor in the vertical direction, was found to be very effective. To provide any evidence of blooming with this system it was necessary to move the camera to within 1 m of the target array, open the lens aperture to $f/2.8$ and set the DX12R flash to full power. Such an exposure setting is some nine stops over that required for optimum exposure and normally only used when imaging the largest retrotargets in this test at distances of over 20 m. The halo just visible at the periphery of this image is attributable to flare caused by the diameter of the ring flash unit being

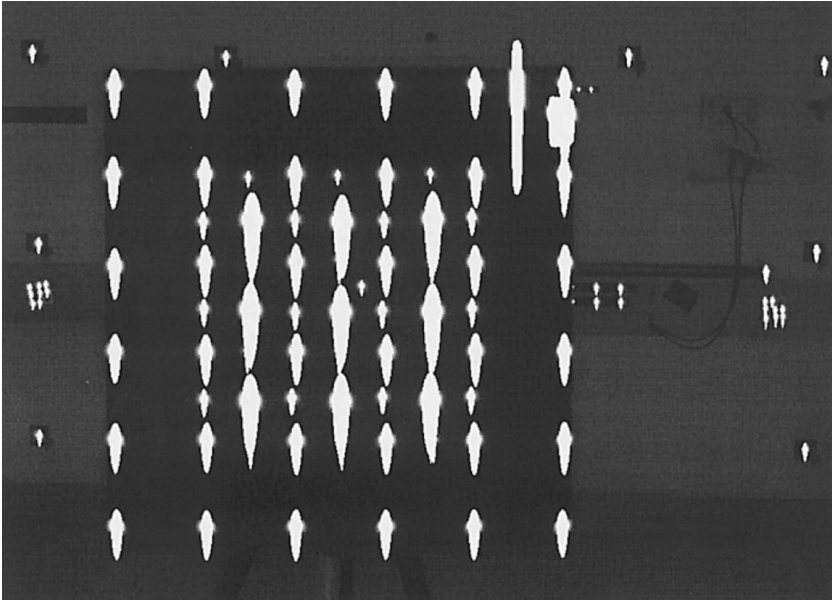


Fig. 6. An extreme case of blooming produced from a CCD array with 100 per cent pixel fill.

insufficient to allow its positioning behind the large front lens element of the 15 mm Nikkor lens.

(ii) *Exposure uniformity tests.* Under practical conditions, it is common practice to vary both lens aperture and ring light illumination to obtain correctly exposed retrotarget images. Images were taken to investigate any variations in target image geometry when lens aperture and electronic shutter duration were varied in sympathy to achieve consistent exposure. Table IIIa contains data pertinent to a set of small sub-images captured with a Kodak MegaPlus ES1.0 camera fitted with a 10 mm f/1.6 Kern Paillard "C" mount lens, whilst Table IIIb represents similar data acquired with a 12.5 mm f/1.4 "C" mount Fujinon lens. The former lens was chosen as it is principally a short focus design and consequently might be expected to have different aberration characteristics to the retrofocus Fujinon lens. Unfortunately, the limited electronic shutter variations possible with the ES1.0 camera only allowed a three stop aperture range to be accommodated for each available level of illumination. However, it is evident from both sets of results that, whilst target images at the centre of the field of view are largely unaffected by aperture variation, those at the format edges vary considerably. The variations seen are attributable to changes in lens aberration brought about by the stopping of paraxial rays as the lens aperture is reduced. The effect of changing the electronic shutter time is not thought to have given rise to any of the observed changes since all shape changes demonstrate distinct radial patterns that are aligned to the centre of the image format.

Object Space Quality Tests

The simple qualitative 2D analysis carried out in the previous section demonstrates significant variation in target image quality that appears consistent with that

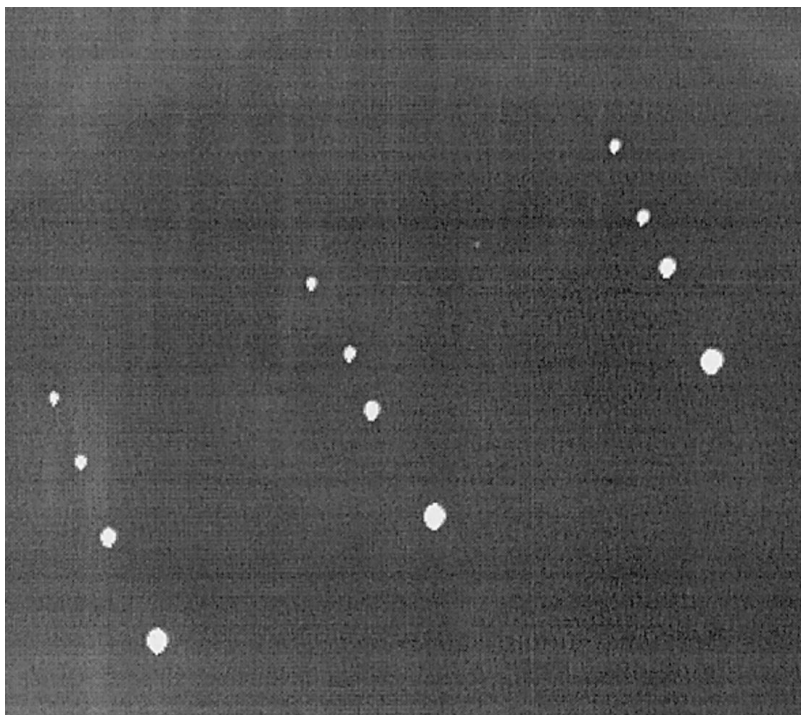


FIG. 7. Probable onset of blooming in an antiblooming array.

expected from lens aberration effects. In order to evaluate the practical significance of some of these factors, a number of network adjustments have been conducted with each camera system. For this initial investigation exposure was varied, by means of electronic flash output, to produce images that contain underexposed, correctly exposed and saturated targets.

Both City University and the University of Melbourne have established retro-target calibration ranges. The current array at City consists of the corner of a laboratory occupying approximately $3 \times 3 \times 3$ m that has been painted matt black. Some 170 retrotargets, 3.2 mm in diameter, are attached to the laboratory wall and ceiling on specially shaped wedges such that all targets are directed towards a notional camera station at the opposite corner of the laboratory. A typical calibration procedure, as replicated in these tests, is to take 12 images from six convergent stations with a 90° roll at each station. Images are then measured and a self-calibrating bundle adjustment computed, a datum being defined by the method of inner constraints, using a research oriented vision metrology package known as VMS, developed jointly by the City University and the University of Melbourne. Two different target arrays at Melbourne were used for these tests. The first consisted of 140 targets attached to a wall and on stands to provide depth, whilst the second was composed of 30 targets located on a mobile $0.6 \times 0.6 \times 0.8$ m calibration trolley. Target diameters for the Melbourne arrays are 9.5 mm and 6.4 mm in the case of the array used for the INCA and DCS cameras and 5 mm in diameter for the Pulnix TM9701 camera networks. The GSI V-Stars package was used to process the INCA and DCS image data, whilst VMS was used for the Pulnix image network.

TABLE IIIa. Variation in both shutter and aperture to maintain a constant exposure. Kodak MegaPlus ES1.0 camera with 10 mm f/1.6 Kern-Paillard "C" mount lens.

Shutter (ms)	f/stop	Background image intensity	Maximum target image intensity	Target image (centre)	Target image (corner)
4	1.6	3	255		
8	2.0	2	255		
16	2.8	2	255		
32	4.0	3	255		

TABLE IIIb. Variation in both shutter and aperture to maintain a constant exposure. Kodak MegaPlus ES1.0 camera with 12.5 mm f/1.4 "C" mount Fujinon lens.

Shutter (ms)	f/stop	Background image intensity	Maximum target image intensity	Target image (centre)	Target image (corner)
4	1.4	3	255(196 corner)		
8	2.0	4	255		
16	2.8	3	255		
32	4.0	2	255		

(i) *Lens distortion curves and lens design characteristics.* Before analysing in detail results from the differing networks, it is useful to consider the radial and tangential lens distortion curves generated for each camera and lens combination. Fig. 8 clearly demonstrates three distinct families of curves. The first, with minimal and very similar distortion, belong to the "F" mount retrofocus design lenses. Second in magnitude are those from the "C" mount lenses. In this set the retrofocus 12.5 mm

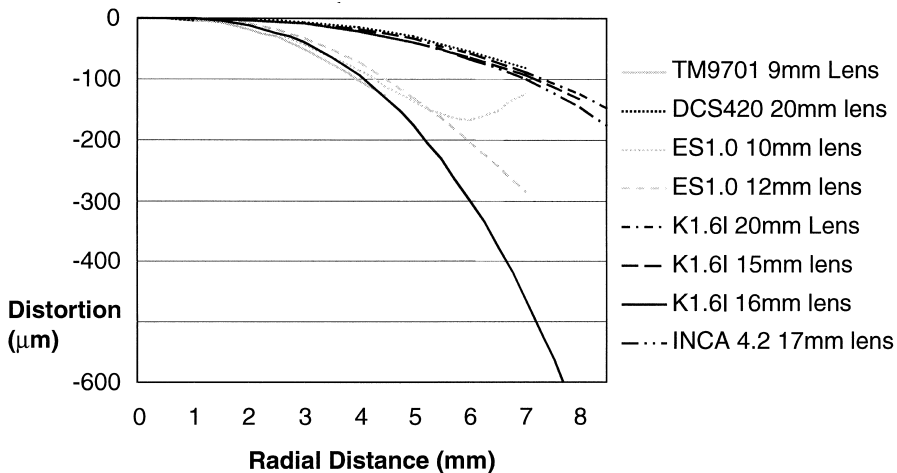


FIG. 8. Radial lens distortion profiles for all evaluated camera and lens combinations.

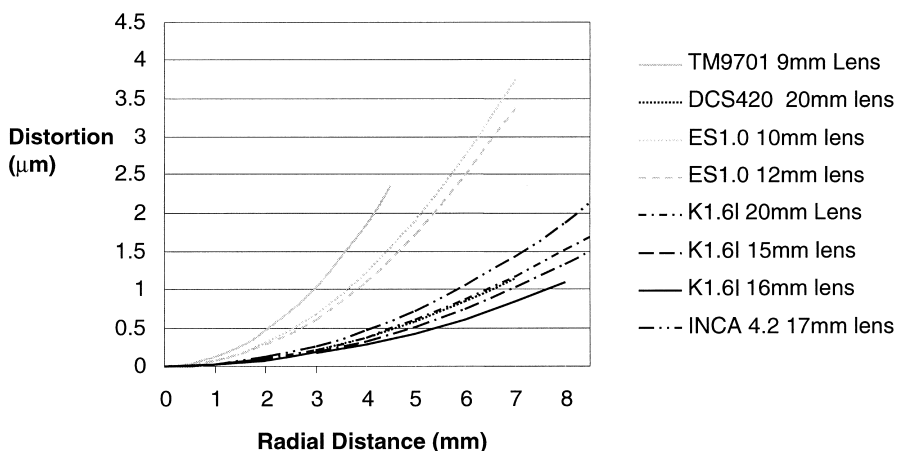


FIG. 9. Tangential lens distortion profiles for all evaluated camera and lens combinations.

and 9 mm Fujinon optics have similar shaped curves, whilst that from the more symmetrical 10 mm Kern-Paillard lens demonstrates greater lens distortion correction towards the edge of the image format. The final curve is computed from the 16 mm quasi-fisheye lens imagery and demonstrates greatly increased radial distortion.

Fig. 9 presents the tangential lens distortion information computed for each network. In this case two distinct groups are paramount with all “F” mount lenses demonstrating consistent and lower distortion than those based on the “C” mount. Again this should be expected as tangential lens distortion is attributable to lens element misalignment and it is likely that alignment of the smaller “C” mount elements is both more critical and more difficult to achieve.

(ii) *Summary of network adjustments.* A subset of results from each calibration series is summarized in Tables IV to XI. For each network the mean camera to object distance was computed and used in conjunction with the physical diameter of the retrotargets in the calibration array to compute predicted target image diameters based on the assumption of collinearity. In every case this diameter was designed to be less than that demonstrated by Dold (1998) as giving rise to significant geometric

TABLE IV. Summary of network adjustment for Kodak ES1-0 camera with Kern-Paillard 10 mm f/1.6 “C” mount lens.

Flash setting	f/stop	Max. grey value	Computed target diameter (pixels)	Mean imaged target diameter (pixels)	Target image centre	Target image edge	Sigma zero	R.m.s. image (µm)	Max. image residual	Object space precision
1				5.4			1.02	0.47	3.30	1:41 000
1/4	11	255	1.1	4.6			1.26	0.57	4.12	1:34 000
1/16				3.5			1.18	0.54	3.45	1:36 500

TABLE V. Summary of network adjustment for Kodak ES1.0 camera with 12.5 mm f/1.4 "C" mount Fujinon lens.





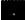

Flash setting	f/stop	Max. grey value	Computed target diameter (pixels)	Mean imaged target diameter (pixels)	Target image centre	Target image edge	Sigma zero	R.m.s. image (μm)	Max. image residual	Object space precision
1				5.8			0.81	0.37	2.45	1:59 500
1/4	11	255	1.4	4.9			1.07	0.49	2.86	1:45 000
1/16				3.9			1.01	0.46	2.55	1:47 500

TABLE VI. Summary of network adjustment for Kodak MegaPlus 1.6I camera with 15 mm f/3.5 "F" mount Nikkor rectilinear lens.





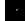

Flash setting	f/stop	Max. grey value	Computed target diameter (pixels)	Mean imaged target diameter (pixels)	Target image centre	Target image edge	Sigma zero	R.m.s. image (μm)	Max. image residual	Object space precision
1		255		7.2			1.01	0.46	3.08	1:52 500
1/4	11	255	1.7	5.5			1.01	0.46	2.27	1:52 500
1/16		212		3.9			0.81	0.37	2.06	1:61 500

TABLE VII. Summary of network adjustment for Kodak MegaPlus 1.6I camera with 16 mm f/2.8 "F" mount Nikkor quasi-fisheye lens.







Flash setting	f/stop	Max. grey value	Computed target diameter (pixels)	Mean imaged target diameter (pixels)	Target image centre	Target image edge	Sigma zero	R.m.s. image (μm)	Max. image residual	Object space precision
1		255		8.5			0.79	0.36	2.49	1:74 500
1/4	11	255	1.8	5.9			0.83	0.38	1.93	1:71 000
1/16		223		4.6			0.65	0.29	1.86	1:83 000

TABLE VIII. Summary of network adjustment for a Kodak MegaPlus 1.6I camera with 20 mm f/2.8 "F" mount Nikkor rectilinear lens (City University network).







Flash setting	f/stop	Max. grey value	Computed target diameter (pixels)	Mean imaged target diameter (pixels)	Target image centre	Target image edge	Sigma zero	R.m.s. image (μm)	Max. image residual	Object space precision
1		255		8.2			1.10	0.49	2.99	1:46 000
1/4	11	255	2.2	5.6			1.03	0.46	2.76	1:49 500
1/16		252		4.2			0.95	0.42	1.89	1:53 500

TABLE IX. Summary of network adjustment for a Kodak DCS420 camera with 20 mm f/2.8 "F" mount Nikkor lens (University of Melbourne network) computed with GSI V-Stars.




Flash setting	f/stop	Max. grey value	Back-ground level	Computed target diameter (pixels)	Mean imaged target diameter (pixels)	Typical target images	R.m.s. image (μm)	Rejected target images	Object space precision
1	8	255	40	3.7	6.1, 9.5		0.46	19	1:16 000
1/4	8	255	27	and	5.8, 8.8		0.16	11	1:48 000
1/16	16	175	25	7.4	5.4, 7.8		0.21	10	1:34 000

TABLE X. Summary of network adjustment for an INCA Megaplus 4.2i Camera with Japanese 17 mm f/3.5 fixed focus lens (University of Melbourne network) computed with GSI V-Stars.

Flash setting	f/stop	Max. grey value	Back-ground level	Computed target diameter (pixels)	Mean imaged target diameter (pixels)	Typical target images	R.m.s. image (μ m)	Rejected target images	Object space precision
2	3.5	255	7	4.7	12.3, 18.6		0.96	75	1:23 500
0	3.5	255	3	and	7.2, 14.2		0.24	35	1:100 000
0	5.6	255	2	9.4	6.5, 12.8		0.16	11	1:133 000
0	8	190	2				0.19	5	1:133 000

TABLE XI. Summary of network adjustment for an Pulnix 9701 Progressive Scan Camera with a Fujinon 9 mm f/1.4 lens (University of Melbourne network).

f/stop	Max. grey value	Back-ground level	Computed target diameter (pixels)	Mean imaged target diameter (pixels)	Typical target images	R.m.s. image (μ m)	Object space precision
2.8	255	12		4.5		1.16	1:9000
5.6	255	11	2.8	4.1		1.42	1:6000
11	170	11		3.1		0.80	1:18 000

differences between the centroid of imaged ellipsoids and the true optical target centre.

There are two major differences between network adjustments carried out at City and those at Melbourne. Firstly, the City testfield is inherently more three dimensional than those used at Melbourne in that targets are spread out over a range of distances in all three dimensions rather than at a pair of discrete depths. Secondly, the target diameters used at City are designed to be of the same order as the resolution limit of the camera systems in order to minimize geometric effects. Those at Melbourne are larger and are probably representative of typical diameters used by commercial systems for practical applications. It should be noted that the collinearity based computation of target size assumes only a mathematical point to point projection. The imaging process generally gives rise to a spreading of light with the result that all imaged target diameters are considerably larger than those computed. This is especially true of those images from the City networks where imaged target size demonstrates considerable variation with electronic flash output. Further, by analysing target images from each of the City networks, it is possible to detect distinct asymmetries in target image geometry that vary with radial distance and lens type. Some of these variations are demonstrated in Tables IV through to VIII under the column heading "target image edge". Similar variations in the Melbourne imagery are also apparent but are of lower magnitude provided that blooming and readout noise remain insignificant.

Tables IV and V summarize adjustments carried out with the Kodak ES1.0 camera in single tap mode with 10 mm and 12.5 mm lenses respectively. With both of these configurations, imaged target diameter is a function of exposure since the small targets are not resolvable without appropriate retarget illumination. In both of these tables, it is readily apparent that edge targets exhibit significant and systematic geometric differences attributable to optical aberration. The edge targets in

Table IV have been extracted from the top right quadrant of the image, whilst those in Table V have been taken from the top left. Within each table all networks and observations are similar with an a priori variance factor of unity. Consequently sigma zero, the a posteriori estimate of unit weight or square root of the variance factor, can be regarded as representing a global adjustment quality measure within each group. For both of the ES1.0 data sets, the quality of each adjustment improves with mean imaged target diameter. This is to be expected within this set as subpixel accuracy is dependent on a minimum target image diameter greater than a few pixels.

Tables VI and VII summarize the network adjustments carried out using a Kodak MegaPlus 1.6I camera fitted with a 15 mm f/3.5 "F" mount Nikkor rectilinear lens and a 16 mm f/2.8 "F" mount Nikkor quasi-fisheye lens respectively. In this case, it is apparent that the images taken with the 15 mm lens exhibit greater target image geometry changes across the format than those made with the 16 mm fisheye lens. In direct comparison with the ES1.0 data, the smaller unsaturated target images with diameters of between four and five pixels are those required to produce optimum network precisions. Given otherwise identical networks, this can only be attributable to more consistent target image shape. Similar results are seen for the 20 mm rectilinear lens (Table VIII), but due to its less extreme lens design, variations in target image geometry are not as obvious nor as influential in terms of adjustment precision.

All images taken as part of the University of Melbourne network testing have been made with larger targets that give rise to computed target image diameters of between three and ten pixels. As a consequence, results from these adjustments exhibit much reduced influence from variations attributable to lens aberration. Instead clear trends in most data sets indicate the effects of flare, read out and blooming.

The adjustments with the DCS420 and GSI INCA cameras have been measured and computed using GSI V-Stars software. Integrated within the V-STARS adjustment is an automated image measurement rejection procedure. This procedure removes image observations from the adjustment if their computed residual is greater than a factor based on the r.m.s. image error. The aim of this is to remove outlying image observations such as those attributable to partially obscured target images. However, it should be noted that unless this procedure is linked to information about target image quality and location within the image format it cannot reliably distinguish between good and bad observations. A similar procedure is available in the VMS software used for the City networks but to simplify this investigation the feature was turned off.

From Tables IX and X, which are derived from sets of adjustments incorporating a dozen frames from six convergent stations, it can be seen that the highest adjustment precisions are achieved with saturated target images. If exposures a little above saturation are made, blooming becomes paramount, particularly for the INCA system as its 4.2I sensor has a 100 per cent pixel fill factor and no antiblooming. Significant read out and blooming are seen in the first two INCA networks where performance is seriously impaired despite automated rejection. Such effects, if not eliminated by careful control of exposure and subsequent analysis of retarget image shape, can be expected to have serious accuracy repercussions as the r.m.s. object co-ordinate discrepancy between the first and last INCA networks was found to be 0.8 mm. It must, however, be stressed that this camera system appears capable of excellent results provided that retarget image quality is carefully monitored.

The Pulnix TM9701 camera used in these investigation forms a part of a work cell configuration being used as a research testing facility at the University of Melbourne. In this case, 10 frames were taken from six convergent stations and a central station with four orthogonal rolls. The 34 imaged targets are arranged in two planes on a calibration trolley. In all cases, despite optimum exposure, significant

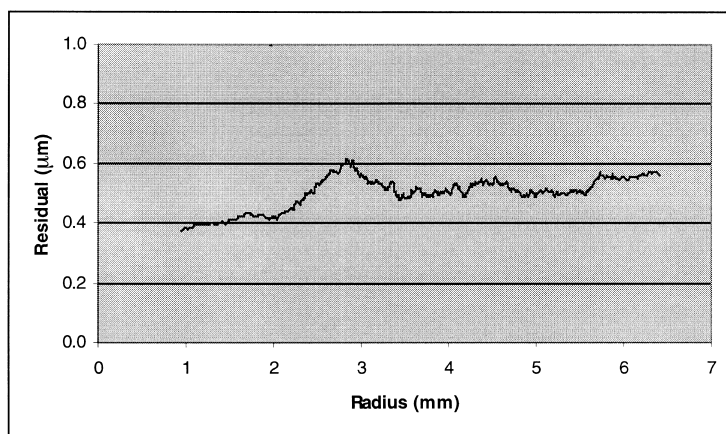


FIG. 10. Moving average radial adjustment residual profile for 20 mm lens.

readout and in some cases blooming is apparent in the target images (Table XI). This has resulted in very low object space precisions, even for targets imaged with a maximum intensity of 170 grey values.

(iii) *Some effects of radial errors attributable to systematic variations in target image shape.* The images from the City networks demonstrate significant systematic target image geometry changes with radial distance. Such effects are not prevalent in the Melbourne networks. Whilst further experimentation is required, it is thought that this difference is attributable to and enhanced by two major causes:

- (a) the very small diameter of the City retrotargets that are imaged at the resolution limit of the camera systems employed; and
- (b) the very low background level of the City images which is between 0 and 2 grey values for all of the images used in the network adjustment tests.

Since the physical effects seen are predominantly radial, an analysis of the residuals from each network adjustment could be expected to demonstrate systematic trends if the radial effect is not adequately modelled within the bundle adjustment process by lens distortion parameters. Figs. 10, 11 and 12 are plots of the moving average of the radial component of all image residuals from all of the adjustment sets for the 20 mm, 15 mm and 16 mm lenses, respectively. In each case, the radial component of the photo-ordinate residuals of each target image location has been computed then smoothed by computing sequential sets of 100 radial image residuals. If no significant systematic effects or signal are present, the expectation would be a horizontal line. In the case of Fig. 10 corresponding to the 20 mm rectilinear lens, it can be seen that whilst there is a slight upward trend any unmodelled radial effects are within the $0.2 \mu\text{m}$ band. The cause of the peak at a radius of 2.5 mm to 3.0 mm in the residual profile for the 20 mm lens is unknown. Fig. 11 is derived from the 15 mm rectilinear lens adjustment data. In this case there is a significant increase in unmodelled radial distortion approaching $0.6 \mu\text{m}$ or $1/15\text{th}$ of a pixel on the 1.6l AB sensor. The greater signal in this case is expected since the extreme design of the 15 mm optic demonstrated significant aberration effects in both 2D and 3D tests. Fig. 12 presents the results for the 16 mm fisheye optic. Here the signal is less extreme than that of

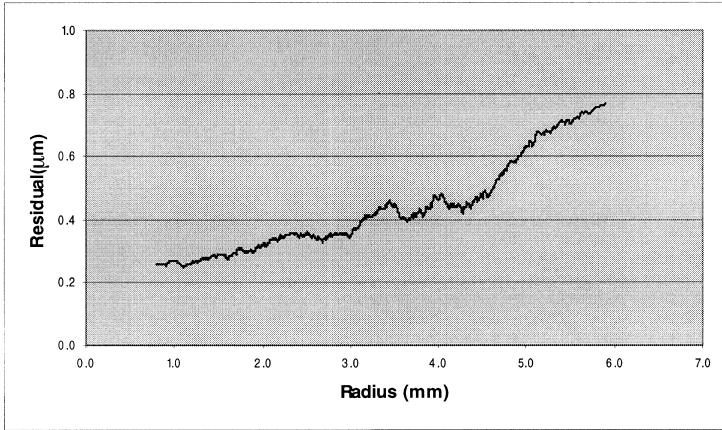


FIG. 11. Moving average radial adjustment residual profile for 15 mm lens.

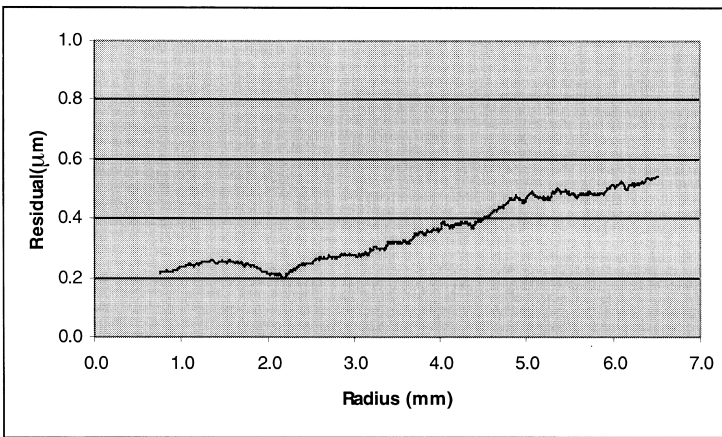


FIG. 12. Moving average radial adjustment residual profile for 16 mm lens.

the 15 mm lens amounting to $0.4 \mu\text{m}$. A much more detailed analysis of the physical cause of these effects is necessary before conclusions can be drawn but any residual systematic effects can be expected to give rise not only to a degradation of adjustment precision but also to a significant and unpredictable worsening of accuracy.

CONCLUSIONS AND FURTHER WORK

Whilst extending both the ease of use and attainable measurement quality using target based techniques, the increasing image quality offered by digital cameras is exposing discrepancies in our understanding and ability to model the photogrammetric process. This paper has identified that optical aberration, CCD blooming and readout can give rise to several largely unmodelled but significant sources of error.

These errors, if present at a significant level, are difficult to remove effectively within the bundle adjustment process. Established rejection procedures based on abnormal target image shape detectors and the automated rejection of abnormal observations can significantly improve the quality of an adjustment, but cannot replace information lost though poor initial imagery.

From the experimental evidence collected so far, it is possible to make preliminary recommendations concerning the use and choice of digital camera systems for high precision photogrammetric use. However in applying these recommendations to practical situations, it should be remembered that the work conducted for this paper has pushed the systems outside the image quality constraints that are associated with good photogrammetric practice.

Given the performance of the lenses tested in this paper and the photogrammetrist's continued use of "off the shelf" optics, it is recommended that careful testing and verification is required before any individual lens system is used to make measurements that are designed to achieve very high accuracies. Also important is justification of a choice of sensor with minimal antiblooming, as optimal results are achieved at or just below saturation, which in such sensors may invite read out and blooming effects. The combination of these and other effects must therefore be routinely monitored or controlled by a careful choice and understanding of optical performance, exposure control and, if appropriate, by the inclusion of CCD sensor antiblooming features at the expense of pixel fill factor. Particular emphasis must also be placed upon the simple planar tests that demonstrated that optical aberrations associated with differences between the imaging characteristics of axial and paraxial rays can give rise to significant differences in imaged target shape with change in aperture. Whilst such changes can again be minimized in practice by the adoption of carefully designed working procedures, the detection of any target shape change with aperture infers that significant lens aberration is present.

Comparison between the 16 mm quasi-fisheye lens and the equivalent 15 mm rectilinear lens demonstrates that, provided that retotargets are the primary image content, the fisheye design is capable of providing superior target image measurement precision when compared to extreme rectilinear wide angle designs. The quasi-fisheye lens realizes favourable results attributable to a lessening of target image ellipticity and more even illumination across the format.

The observed physical differences in target image shape between the City and correctly exposed Melbourne networks require further investigation. At this stage, it can only be reasonably concluded that, whilst small target sizes will minimize the effect of ellipsoidal imagery when using centroid algorithms, their imaged size must be large enough to provide sufficient image information and must not be so small that lens aberration effects become paramount. Research is therefore required utilizing a range of target sizes and rigorous accuracy testing to reliably quantify and categorize both the physical causes and practical significance of the effects described in this paper. Further, in cases where aberration effects are significant it should be possible to combine a knowledge of lens design and established mathematical models for Seidel aberrations to efficiently account for the systematic effects demonstrated in this paper.

REFERENCES

- ARNOLD, C. R., ROLLS, P. J. and STEWART, J. C. J., 1971. *Applied photography*. Focal Press, London. 510 pages.
- BALTSAVIAS, E., 1991. *Multiphoto geometrically constrained matching*. Ph.D. Dissertation, Institute for Geodesy and Photogrammetry, ETH Zurich. Mitteilungen 49. 221 pages.
- BEYER, H. A., 1995. Digital photogrammetry in industrial applications. *International Archives of Photogrammetry and Remote Sensing*, 30(5W1): 373–378.
- BÖSEMANN, W. and SINNREICH, K., 1994. An optical 3D tube measurement system for quality control in industry. *Automated 3D and 2D vision*. SPIE 2249: 192–199.

- BROWN, D. C., 1984. *A large format, microprocessor controlled film camera optimized for industrial photogrammetry*. Presented paper, XV International Congress of Photogrammetry and Remote Sensing, Rio de Janeiro. 29 pages.
- BROWN, J. and DOLD, J., 1995. V-STARS—a system for digital industrial photogrammetry. *Optical 3D Measurement Techniques III* (Eds. A. Gruen and H. Kahmen). Wichmann, Heidelberg. 533 pages: 12–21.
- CLARKE, T. A., ROBSON, S., QU, D. N., WANG, X., COOPER, M. A. R. and TAYLOR, R. N., 1995. The sequential tracking of targets in a remote experimental environment. *International Archives of Photogrammetry and Remote Sensing*, 30(5W1):80–85.
- DOLD, J., 1996. Influence of large targets on the results of photogrammetric bundle adjustment. *Ibid.*, 31(B5): 119–123.
- DOLD, J., 1998. The role of a digital intelligent camera in automating industrial photogrammetry. *Photogrammetric Record*, 16(92): 199–212.
- FRASER, C. S. and SHORTIS, M. R., 1995. Metric exploitation of still video imagery. *Ibid.*, 15(85): 107–122.
- GRANSHAW, S. I., 1980. Bundle adjustment methods in engineering photogrammetry. *Ibid.*, 10(56): 181–207.
- GRUEN, A. W. and BALTSAVIAS, E. P., 1988. Geometrically constrained multiphoto matching. *Photogrammetric Engineering and Remote Sensing*, 54(5): 633–641.
- HAGGRÉN, H. and HAAJANEN, L., 1990. Target search using template images. *International Archives of Photogrammetry and Remote Sensing*, 28(5/1): 572–578.
- VAN DEN HEUVEL, F. A., KROON, R. J. G. A. and LE POOLE, R. S. 1992. Digital close-range photogrammetry using artificial targets. *Ibid.*, 29(5): 222–229.
- HORI, T., 1995. Progressive scan interline transfer CCD camera. *Cameras and systems for electronic photography and scientific imaging*. SPIE 2416: 17–29.
- KODAK, 1995. *Kodak Megaplug Camera, Model 1.4, expanded specification revision A*. Motion Analysis Systems Division, Eastman Kodak Company, Rochester, New York. 35 pages.
- KRAUS, K., 1993. *Photogrammetry. Volume 1. Fundamentals and standard processes*. Dümmler, Bonn. 397 pages.
- LENZ, R. and FRITSCH, D., 1988. On the accuracy of videometry. *International Archives of Photogrammetry and Remote Sensing*, 27(B5): 335–345.
- POL, V., BENNEWITZ, J. H., JEWELL, T. E. and PETERS, D. W., 1987. Excimer laser based lithography: a deep-ultraviolet wafer stepper for VSLI processing. *Optical Engineering*, 26(4): 311–315.
- RAY, S. F., 1994. *Applied photographic optics*. Second edition. Focal Press, Oxford. 586 pages.
- RAYNOR, J. M. and SEITZ, P., 1990. The technology and practical problems of pixel-synchronous CCD data acquisition for optical metrology applications. *International Archives of Photogrammetry and Remote Sensing*, 28(5): 96–103.
- ROBSON, S., CLARKE, T. A. and CHEN, J., 1993. The suitability of the Pulnix TM6CN CCD camera for photogrammetric measurement. *Videometrics II*. SPIE 2067:66–77.
- SHORTIS, M. R. and BEYER, H. A., 1996. Sensor technology for digital photogrammetry and machine vision. *Close range photogrammetry and machine vision* (Ed. K. B. Atkinson). Whittles Publishing, Caithness. 371 pages: 106–155.
- SHORTIS, M. R. and BEYER, H. A., 1997. Calibration stability of the Kodak DCS420 and 460 cameras. *Videometrics V*. SPIE 3174: 94–105.
- SHORTIS, M. R., CLARKE, T. A. and ROBSON, S., 1995. Practical testing of the precision and accuracy of target image centering algorithms. *Videometrics IV*. SPIE 2598: 65–76.
- SHORTIS, M. R., CLARKE, T. A. and SHORT, T. 1994. A comparison of some techniques for the subpixel location of discrete target images. *Videometrics III*. SPIE 2350: 239–250.
- SHORTIS, M. R., SNOW, W. L. and GOAD, W. K., 1995. Comparative geometric tests of industrial and scientific CCD cameras using plumb line and test range calibrations. *International Archives of Photogrammetry and Remote Sensing*, 30(5W1): 53–59.
- STANTON, R. H., ALEXANDER, J. W., DENNISON, E. W., GLAVICH, T. A. and HOVLAND, L. F., 1987. Optical tracking using charge-coupled devices. *Optical Engineering*, 26(9): 930–935.
- TRINDER, J. C., 1989. Precision of digital target location. *Photogrammetric Engineering and Remote Sensing*, 55(6): 883–886.
- WELFORD, W. T., 1974. Film flatness, lens distortion, illumination and other matters in bubble chamber photography. *Photogrammetric Record*, 8(44): 167–177.
- ZHOU, G., 1986. Accurate determination of ellipse centers in digital imagery. *Technical Papers*, Volume 4, ACSM-ASPRS Annual Convention, Washington D.C. 519 pages: 256–264.

Résumé

Les systèmes imageurs basés sur la technologie actuelle des caméras numériques, sont d'un usage très répandu dans les applications nécessitant des déterminations de haute précision. On utilise couramment les caméras

numériques à DTC, soit isolément, soit disposées en rangée, avec leur dispositif d'éclairage en anneau, pour saisir l'image de cibles réfléchissantes à grand contraste placées sur les objets à des emplacements bien définis permettant de matérialiser des points caractéristiques. Il faut effectuer avec précision et exactitude la mesure des positions des images de chaque cible si l'on veut respecter des tolérances convenables sur les objets. Même si l'on peut obtenir sans aucun doute d'excellents résultats avec de tels systèmes, il n'est pas inutile de prêter attention à l'influence pratique de la qualité de l'image des cibles sur le processus de détermination photogrammétrique. Après un rappel de quelques propriétés optiques concernées dans l'obtention de l'image de cibles réfléchissantes, on examine dans cet article les possibilités de toute une gamme de systèmes à caméras numériques à fournir des images de ces cibles qui conviennent tout à fait au processus de mesure. On présente également quelques résultats expérimentaux, comprenant ceux où l'on a mis en œuvre des matrices planes de mires réfléchissantes de différentes tailles, vues sous différents angles, avec différentes expositions, ainsi qu'une série d'analyse d'un réseau où l'on a fait varier systématiquement le niveau de l'intensité de l'image de la mire.

Zusammenfassung

Abbildende Systeme, die auf der gegenwärtigen Technologie digitaler Kameras beruhen, sind bei hochpräzisen Meßanwendungen weitverbreitet. Eine einzelne digitale CCD-Kamera oder ein Verband solcher Kameras, die mit einer Ringblitzeinrichtung ausgestattet sind, werden in der Regel genutzt, um kontrastreiche Abbildungen von selbstreflektierenden Zielzeichen am Objekt, mit denen diskrete Positionen zur Signalisierung von interessierenden Punkten bezeichnet werden, zu gewinnen. Die genaue Messung jedes markierten Zielpunktes ist eine fundamentale Anforderung, wenn geeignete Meßtoleranzen erhalten werden sollen. Während solche Systeme zweifelsohne vorzügliche Ergebnisse liefern können, muß den praktischen Einflüssen der Abbildungsqualität der Zielzeichen auf den photogrammetrischen Meßprozeß sorgfältige Beachtung geschenkt werden. Daher werden einige Grundlagen der optischen Abbildung von Retrozielzeichen aufgefrischt und die Eigenschaften einer Reihe von Digitalkameras zur Erzeugung von Bildern von selbstreflektierenden Zielmarken, die für den Meßprozeß geeignet sind, untersucht. Einige experimentelle Ergebnisse werden angegeben, darunter die Abbildung ebener Anordnungen von Retrozielmarken unterschiedlicher Größe unter verschiedenen Winkeln und bei unterschiedlichen Belichtungen und eine Serie von Netzwerkanalysen, bei denen die Intensität des Zielmarkenbildes systematisch verändert wurde.